Noninvasive Assessment of the Complexity and Stationarity of the Atrial Wavefront Patterns During Atrial Fibrillation

Pietro Bonizzi*, María de la Salud Guillem, Andreu M. Climent, Jose Millet, Vicente Zarzoso, *Member, IEEE*, Francisco Castells, and Olivier Meste

***Abstract*—A novel automated approach to quantitatively evaluate the degree of spatio-temporal organization in the atrial activity (AA) during atrial fibrillation (AF) from surface recordings, obtained from body surface potential maps (BSPM), is presented. AA organization is assessed by measuring the reflection of the spatial complexity and temporal stationarity of the wavefront patterns propagating inside the atria on the surface ECG, by means of principal component analysis (PCA). Complexity and stationarity are quantified through novel parameters describing the structure of the mixing matrices derived by the PCA of the different AA segments across the BSPM recording. A significant inverse correlation between complexity and stationarity is highlighted by this analysis. The discriminatory power of the parameters in identifying different groups in the set of patients under study is also analyzed. The obtained results present analogies with earlier invasive studies in terms of number of significant components necessary to describe 95% of the variance in the AA (four for more organized AF, and eight for more disorganized AF). These findings suggest that automated analysis of AF organization exploiting spatial diversity in surface recordings is indeed possible, potentially leading to an improvement in clinical decision making and AF treatment.**

***Index Terms*—Atrial fibrillation (AF), body surface potential mapping (BSPM), cluster analysis, principal component analysis (PCA), singular value decomposition (SVD), spatial topographies.**

I. Introduction

DURING atrial fibrillation (AF), the atrial tissue is activated by multiple wavelets showing uncoordinated patterns, appearing as an irregular heart rhythm disturbance with no detectable relationship between consecutive beats. For this reason, AF has often been studied as a random phenomenon [1], [2]. Nonetheless, several studies have demonstrated the presence of organization of atrial activation processes during AF, indicating that a certain degree of local organization exists during AF, likely caused by deterministic mechanisms of activation [3], and inversely depending on the chronification of the pathology [4]. Moreover, several authors have observed that different types of AF patterns could be concurrently present at different locations during experimental AF [5], [6]. Hence, from a pathophysiological point of view, it can be inferred that AF is not a homogeneous arrhythmia [7]. Different strategies for its treatment are selected with respect to the duration of its episodes [8], and their efficacy may also be influenced by the degree of organization in the atrial activity (AA) [9].

Motivated by their potential relevance in clinical decision making, a number of earlier studies have attempted to distinguish between organized and disorganized states of AF by analyzing atrial electrograms [10], [11]. Konings *et al.* [11], in the attempt of reconstructing and classifying the patterns of human right atrial activations during electrically induced AF, defined three types of AF based on the degree of complexity of atrial activations. An increasing fractionation of the observed atrial activations was associated with an increasing number of interacting wavefronts and thus a higher complexity. Faes *et al.* [12] used principal component analysis (PCA) in order to quantify the number of dominant components in the atrial activations, as an estimate of AA complexity. These authors [12] noticed that single-lead electrograms recorded at different sites and presenting different AA organization were shown to be represented by a different number of principal components (PCs), with a reduced number of components representing more organized AA [12].

On the other hand, surface ECG has been demonstrated to be a valuable cost-effective tool for studying AF [13]. Hence, more recent studies [14] have attempted a noninvasive evaluation of AF organization through ECG recordings, demonstrating the possibility of visually evaluating different activation patterns in AF patients, similar to those observed invasively by Konings *et al.* [11], although applied to surface recordings instead of electrograms. Body surface potential maps (BSPM) [15] have also been earlier applied to the study of many cardiac diseases [16], [17], and have the advantage over the conventional ECG of a much higher spatial resolution. Using BSPM, Guillem *et al.* [14] have observed interindividual differences of surface

Manuscript received November 26, 2009; revised March 11, 2010 and May 27, 2010; accepted May 28, 2010. Date of publication June 14, 2010; date of current version August 18, 2010. The work of P. Bonizzi was supported by the EU by a Marie–Curie Fellowship (EST-SIGNAL program: http://est-signal.i3s.unice.fr) under Contract MEST-CT-2005-021175. The work of M. de la Salud Guillem, A. M. Climent, and F. Castells was supported by a Spanish Ministry of Science and Innovation under Contract TEC2008-02193/TEC. *Asterisk indicates corresponding author.*

*P. Bonizzi is with the Laboratoire d'Informatique, Signaux et Systèmes de Sophia Antipolis (I3S), Université de Nice Sophia Antipolis/Centre National de la Recherche Scientifique, Sophia Antipolis, 06903 France (e-mail: bonizzi@i3s.unice.fr).

M. de la Salud Guillem, A. M. Climent, J. Millet, and F. Castells are with the Biomedical Engineering Branch, Institute for Applications of Advanced Information and Communication Technologies, Universitat Politecnica de Valencia, 46022 España, Spain (e-mail: mariaguillem@gmail.com; bamarcli@gmail.com; jmillet@eln.upv.es; fcastells@eln.upv.es).

V. Zarzoso and O. Meste are with the Laboratoire d'Informatique, Signaux et Systèmes de Sophia Antipolis (I3S), Université de Nice Sophia Antipolis/Centre National de la Recherche Scientifique , Sophia Antipolis, 06903 France (e-mail: zarzoso@i3s.unice.fr; meste@i3s.unice.fr).

Digital Object Identifier 10.1109/TBME.2010.2052619

atrial fibrillatory activation patterns characterized by an excellent short-term reproducibility.

In line with this study, the present work puts forward a new automated method for noninvasively evaluating the degree of spatio-temporal organization of atrial activations during AF. By means of PCA, AA organization is evaluated quantitatively on one hand by assessing the spatial complexity of the recorded surface atrial waveforms and on the other hand by assessing the temporal stationarity of the AA potential field pattern from the analysis of BSPM recordings. PCA has been attested to be a valuable tool both for addressing diverse issues in ECG analysis [18], and for quantifying AA organization complexity in invasive recordings [12]. Moreover, the spatial information derivable from the PCA of the different ECG components in a multi-lead recordings has turned out to be useful as a first step in the extraction of the AA from surface ECG [19], [20]. Hence, complexity and stationarity are quantified herein with novel parameters that assess the structure of the mixing matrices derived from the PCA of the different AA segments in the BSPM recording. Furthermore, the discriminatory power of these parameters in identifying different groups of patients in the dataset under study is explored. Results are then compared to earlier invasive studies, highlighting interesting analogies and suggesting their physiological interpretation, together with their potential usefulness in clinical applications. The paper is outlined as follows: the method is presented in Section II, the results in Section III, and their discussion is found in Section IV. Finally, conclusions are given in Section V.

II. Materials and Methods

A. BSPM Data and Acquisition System

The same dataset composed of 14 patients as the one introduced in [14] was employed in this study (ten males, four females; age 68 ± 14 years; AF duration 12 ± 18 months). Patients were receiving different pharmacological treatments, and some of them were affected by additional heart disease, like hypertension or coronary heart diseases. One BSPM signal was recorded for each patient. All recordings presented persistent AF. The acquisition system consisted of a total of 56 chest and back leads acquired simultaneously for each subject. Chest leads ($n = 40$) were arranged as a uniform grid around V1 with an interelectrode distance of 2.2 cm, while back leads ($n = 16$) were arranged in a similar way around a lead opposite to V1 (V1post), as shown in Fig. 1(a). Only the first 60 s of each BSPM recording were analyzed in this study.

Signals were acquired at a sampling frequency of 2048 Hz, with a resolution of 1 μV and filtered with an antialiasing low-pass bandwidth of DC-500 Hz.

B. ECG Signal Preprocessing

Signals were processed by applying a third-order zero-phase high-pass Chebyshev filter with a -3 dB cutoff frequency at 0.5 Hz to remove baseline wandering due to physiologically irrelevant low-frequency signal interference (<1 Hz), like breathing influence [21]. That was followed by a third-order zero-phase low-pass Chebyshev filter with a -3 dB cutoff frequency at 100 Hz to remove high-frequency noise, like myoelectric artifacts. Finally, a zero-phase notch filter at 50 Hz was used to suppress power-line interference.

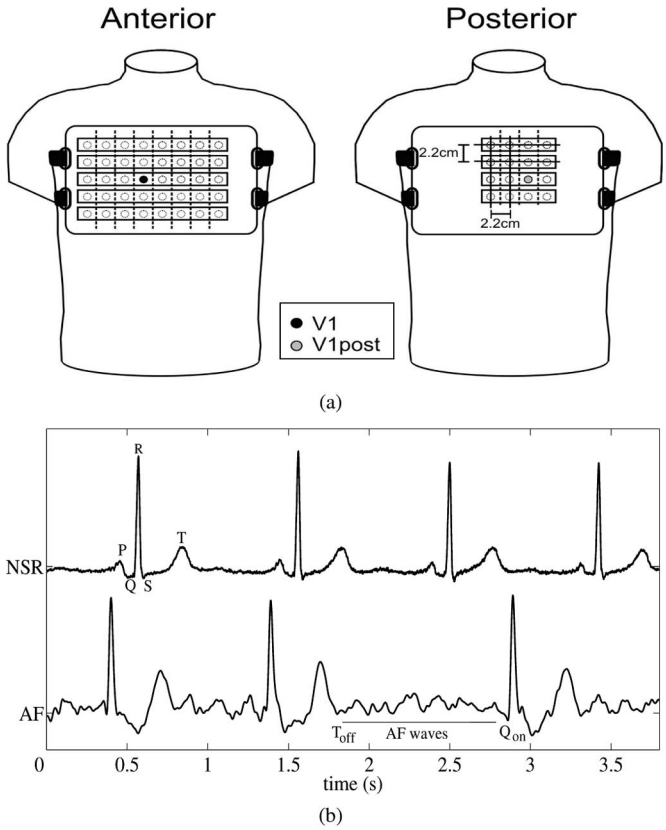

Fig. 1. (a) Arrangement of the electrodes and belt used for their attachment to the patient. Electrode positions are represented as open circles while V1 and V1post are denoted by black and gray circles, respectively. Electrodes were placed around V1 and V1post as a uniform grid. (b) Definition of the different cardiac waves and intervals of interest. At the top, example of normal sinus rhythm ECG recording, showing the different cardiac waves. At the bottom, example of ECG recording during AF, showing a TQ interval (off:offset; on:onset).

All leads in all recordings were visually inspected. Leads presenting noticeable noise contributions, typically due to a transient loss of contact in one electrode, were discarded. This preserved the following PCA from being impaired by the abnormal statistical behavior of these observations. Since the average of discarded leads was 1 per recording, and taking into account the large number of leads at our disposal, we considered the number of remaining leads sufficient for subsequent analysis, avoiding the interpolation of the discarded leads.

C. AA Recordings

In this study, only TQ segments in the BSPM recording were analyzed. For this purpose, the R-wave peaks were detected, and the Q-wave onset and T-wave offset were properly segmented (see Fig. 1(b) for the definition of the different cardiac waves). Each BSPM lead recording was split in six consecutive 10s-length intervals, and an AA signal was obtained for each interval concatenating only the TQ segments inside it. To

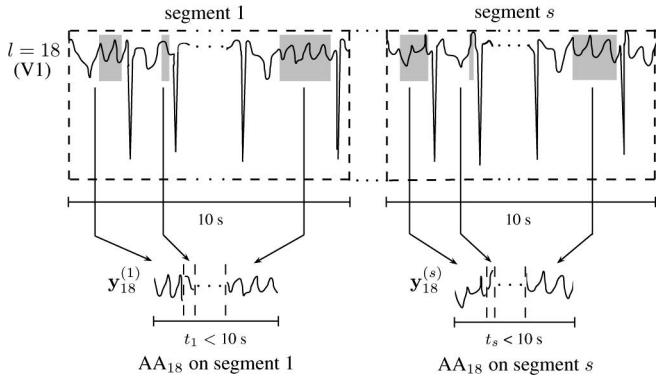

Fig. 2. Schematic example of AA recording generation on lead 18 only (lead V1). Each lead recording is split in consecutive and nonoverlapping 10 s segments, and all TQ intervals inside a specific segment s are joint in order to get the AA recording $\mathbf{Y}^{(s)}$.

accomplish that, lead V1 was selected and the R-wave instants detected using a Pan and Tompkins's QRS detection method [21]. The detection results were visually inspected for each patient, in order to avoid missing detections or artifacts. Then, for each R-wave instant, a suitable window including the QRS-T complex was defined starting 40 ms before the R-wave instant and terminating t_{end} milliseconds after, where $t_{\mathrm{end}} = \min(\mathrm{RR(ms)}) - 40$ ms, and with RR representing the RR period (R-wave to following R-wave interval). Finally, all QRS-T complexes were removed using the introduced window, and all the TQ segments connected together. Additionally, after QRS-T removal, each lead was visually inspected and parts of QRS-T complexes still present further removed, removing the corresponding temporal part from all the other leads. The synchronism of all R-wave instants in all leads, and so of all the windows exploited to remove the QRS-T complexes, guaranteed maintenance of synchronism among leads by the major preprocessing step, guaranteeing PCA to obtain an instantaneous representation of the interaction among the original signals. In this way, for each 56-lead BSPM recording we constructed six consecutive 56-lead AA recordings.

Each lead l in the sth AA recording (with $s = 1, \ldots, 6$) is represented by a row vector

$$\mathbf{y}_l^{(s)} = [y_l^{(s)}(1), \ldots, y_l^{(s)}(N)] \tag{1}$$

where N is the number of samples inside the interval. Then, the entire ensemble of leads is compactly represented by the $56 \times N$ matrix

$$\mathbf{Y}^{(s)} = \begin{bmatrix} \mathbf{y}_1^{(s)} \\ \vdots \\ \mathbf{y}_{56}^{(s)} \end{bmatrix}.$$

A schematic example of this procedure is illustrated in Fig. 2 for the sake of clarity, for lead $l = 18$ only, corresponding to V1.

D. Principal Component Analysis

ECG is a signal with a high spatial redundancy [18]. One manner to analyze the complex information contained in the ECG is to transform the original set of signals in a set of components by minimizing the redundancy among them. This can be achieved by PCA. Indeed, spatial uncorrelation provided by PCA involves a linear transformation of the mean-corrected observed signals $\mathbf{Y} \in \mathbb{R}^n$, which produces a set of mutually uncorrelated waveforms with unit variance $\mathbf{X} \in \mathbb{R}^m$ with $(m \leq n)$. The PCA of $\mathbf{Y}$ yields an estimate of the following noiseless model:

$$\mathbf{Y} = \mathbf{M}\mathbf{X} \Rightarrow \mathbf{X} = \left[\mathbf{M}^{\mathrm{T}}\mathbf{M}\right]^{-1}\mathbf{M}^{\mathrm{T}}\mathbf{Y} = \mathbf{M}^{\sharp}\mathbf{Y} \tag{2}$$

where $\mathbf{X}$ is an estimate of the true vector of the unknown components, $\mathbf{M}$ is the mixing matrix, symbol $(\cdot)^{\mathrm{T}}$ stands for the transpose operator, and symbol $(\cdot)^{\sharp}$ stands for the pseudoinverse operator. Even if the model in (2) is supposed to be noiseless, this model is usually employed in the presence of noise as well. In that case, the number of PCs generally matches the number of measured signals, and the last PCs are associated with noise. The ith column of $\mathbf{M}$ represents the source direction or spatial topography that links the ith component of $\mathbf{X}$ with the observed signals $\mathbf{Y}$. The spatial topography describes the relative contribution of the uncorrelated components to each electrode. That means, each one of its entries reflects the spatial pattern distribution of the relative potential field described by the associated components onto the spatially-separated electrodes. PCA reduces the dataset of the observed signals to few representative components. The mixing matrix $\mathbf{M}$ can be obtained, e.g., from the singular value decomposition of the observation matrix $\mathbf{Y} = \mathbf{U}\mathbf{\Sigma}\mathbf{V}^{\mathbf{T}}$, where $\mathbf{M} = \mathbf{U}\mathbf{\Sigma}/\sqrt{N}$, with matrix $\mathbf{U}$ and $\mathbf{V}$ containing the left and right singular vectors of $\mathbf{Y}$, respectively, and matrix $\mathbf{\Sigma}$ being the diagonal matrix containing the singular values σ_i (≥ 0) at which each PC is associated. σ_i indicates how representative is the ith PC in the global data ensemble. The PCs are usually arranged so that the singular value sequence appears in a decreasing order. This sequence reflects some information regarding interlead variability. In fact, a fast fall-down is associated with a low spatial variability, while a slow fall-down indicates a large spatial variability. Hence, the ability of PCA to concentrate the original information in only k components (number of significant components, $k < m$) can be assessed by the cumulative normalized variance v_k, an index that reflects how well the subset of the first k PCs approximates the ensemble of original observations in energy terms

$$v_k = \frac{\sum_{i=1}^{k}\sigma_i^2}{\sum_{i=1}^{m}\sigma_i^2}. \tag{3}$$

E. Assessment of Spatio-temporal Organization of the AA

The degree of spatio-temporal organization of the AA during AF is noninvasively evaluated as the spatial complexity and temporal stationarity of the wavefront pattern propagating inside the atria, as reflected on the surface ECG. In this paper, spatial complexity describes the spatial multi-lead variety in the waveforms of the recorded surface atrial signals, while temporal stationarity evaluates the preservation of the AA potential field

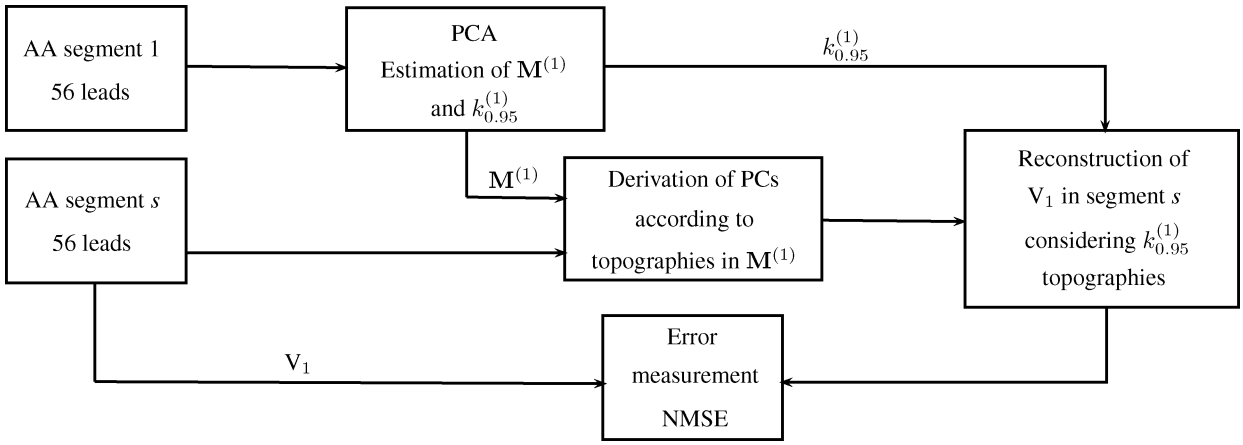

Fig. 3. Block diagram of the proposed procedure. AA recording on the sth segment $\mathbf{Y}^{(s)}$ is projected on the spatial topographies associated with the most significant PCs of the initial segment $\mathbf{M}^{(1)}$, yielding the projection $\hat{\mathbf{Y}}^{(s)}$. $k_{0.95}^{(1)}$: number of significant components describing 95% of the variance of the first segment. NMSE: normalized mean square error.

spatial patterns over the experiment. These two aspects are investigated through the structure of the mixing matrices inferred from PCA of the different AA segments in the BSPM recording, introduced in Section II-C. Complexity is analyzed in terms of the number of components required for explaining 95% of the variance of the underlying AA, while stationarity is quantified in terms of the repetitiveness of the mixing matrix along the BSPM recording, as follows.

1) AA Spatial Complexity: A more organized AA is supposed to be reflected in the structure of the PCA mixing matrix in terms of a lower number of significant components needed to describe its variance. To this end, the average number of significant components k for all segments s required to explain 95% of the variance ($k_{0.95}$) is considered a first indicator of AF organization. More specifically, for a given patient, the PCA of the sth segment yields an estimate of the noiseless model (2)

$$\mathbf{Y}^{(s)} = \mathbf{M}^{(s)}\mathbf{X}^{(s)} \tag{4}$$

and the average number $k_{0.95}$ is derived over all PCA mixing matrices $\mathbf{M}^{(s)}$. The underlying idea is that low complexity describes low morphological variability, whereas higher complexity describes larger morphological variability.

2) AA Temporal Stationarity: To increase the discriminatory power of the analysis, the data in the sth segment are reprojected on the spatial topographies associated with the $k_{0.95}^{(1)}$ most significant PCs of the initial segment (where superscript $^{(1)}$ identifies the first segment), stored in the first k columns of matrix $\mathbf{M}^{(1)}$. This projection can be expressed as

$$\begin{aligned}\hat{\mathbf{Y}}^{(s)} &= \mathbf{M}_k^{(1)}\left[(\mathbf{M}_k^{(1)})^{\mathrm{T}}\mathbf{M}_k^{(1)}\right]^{-1}(\mathbf{M}_k^{(1)})^{\mathrm{T}}\mathbf{Y}^{(s)} \\ &= \mathbf{M}_k^{(1)}(\mathbf{M}_k^{(1)})^{\sharp}\mathbf{Y}^{(s)}.\end{aligned} \tag{5}$$

From this relationship, the normalized error between the data present in the sth segment and their reconstruction from the $k_{0.95}^{(1)}$ most significant topographies of the initial segment is computed. This error measures the temporal stationarity or persistence of the AA potential field pattern in the BSPM recording as the ability of $\mathbf{M}^{(1)}$ derived for the initial segment $\mathbf{Y}^{(1)}$ to retrieve the AA components of subsequent segments. This is related to the propensity of the spatial topographies associated with the first $k_{0.95}^{(1)}$ PCs to keep unchanged over the whole experiment. We assume this measure is inversely proportional to the AF organization, and thus directly to its complexity. Indeed, the closer matrices $\mathbf{M}^{(s)}$ and $\mathbf{M}^{(1)}$ are, the closer the reconstructed observations with the originals are. Hence, more organized states of AF are reflected on an increased repetitiveness of the principal spatial topographies across the surface recording. An example of the procedure is illustrated in Fig. 3.

The reconstruction error is computed in terms of normalized mean squared error ($\mathrm{NMSE}_{k_{0.95}}$) on lead 18, corresponding to V_1 (this is the lead from the standard 12-lead ECG that usually exhibits atrial fibrillatory waves with larger amplitude). In what follows, subscript index 18 is substituted by V1 for clarity:

$$\mathrm{NMSE}_{k_{0.95}}^{(s)} = \frac{\sum_{i=1}^{N}(y_{V1}^{(s)}(i) - \hat{y}_{V1}^{(s)}(i))^2}{\sum_{i=1}^{N}(y_{V1}^{(s)}(i))^2} \tag{6}$$

where $\mathbf{y}_{V1}^{(s)}$ denotes the reference signal, actually measured on V1, $\hat{\mathbf{y}}_{V1}^{(s)}$ an estimate of it, and N their length. High values indicate notable differences between the original and reconstructed AA signals, while values close to zero are associated with very similar AA signals.

In addition to the experiment described earlier, a further study is carried out considering a fixed number of topographies for all patients, instead of $k_{0.95}^{(1)}$. More specifically in this study, we consider $k = 3$, similar to the three most significant components, which are supposed to contain most of the information of the ECG, at least in signals with low complexity [22], [23]. Indeed, some studies claim that the ECG can be well explained using only three components so that just with the first three eigenvectors and eigenvalues, the essential information of the ECG is retained. This property motivated, e.g., the definition of the T-wave residuum [24], which accounts for the proportion of the data that lies out of the aforementioned 3-D space where cardiac signals have been usually represented, such as the vectorcardiogram. The idea behind the study proposed here is that

patients with more organized AA patterns will probably require a lower number of components to represent 95% of the variance in the original data. Similarly, if a small number of components is selected, a better reconstruction is expected for patients with more organized AA patterns. As a result, the reconstruction error is once more computed and defined as $\text{NMSE}_{k=3}$. With this experiment, the effects of the spatial complexity and temporal reproducibility of AA patterns are joined in a single parameter, and therefore, it is expected to emphasize the differences between more organized and less organized AF groups. The procedure is the same as the one shown in Fig. 3, but considering $k = 3$ instead of $k_{0.95}^{(1)}$.

In order to enhance the hypothesis that complexity held in the analyzed signals is really a characteristic related to AA, two additional analyses are carried out. First, the possible influence of the noise on the complexity of the signal is investigated looking at the correlations of both $k_{0.95}$ and $\text{NMSE}_{k=3}$, respectively, with the energy of the AA segments. Second, the correlation between the difference $\text{NMSE}_{k_{0.95}} - \text{NMSE}_{k=3}$ and $k_{0.95}$ is investigated in order to test the influence of the method on the increase of the correlation between complexity and NMSE when fixing $k = 3$.

F. Cluster Analysis

The spatio-temporal analysis presented in Section II-E, can be seen as a new way for noninvasively assessing the degree of spatio-temporal organization of the AA during AF. Consequently, it appears worthy to investigate the ability of the proposed parameters to identify different clusters in the dataset under analysis. To this end, the discriminatory power of $k_{0.95}$, $\text{NMSE}_{k_{0.95}}$, $\text{NMSE}_{k=3}$ is individually considered, and of the two combinations $k_{0.95}$, $\text{NMSE}_{k_{0.95}}$ and $k_{0.95}$, $\text{NMSE}_{k=3}$ is analyzed, performing five cluster analysis on the whole dataset (the combination $\text{NMSE}k_{0.95}$ with $\text{NMSE}_{k=3}$ was considered of no particular meaning, since these two parameters are strongly related). A K-means algorithm for clustering is used, based on an iterative partitioning that minimizes the sum, over all clusters, of the within-cluster sums of point-to-cluster-centroid distances. The standard metric chosen is the squared Euclidean distance

$$d = \sum_{j=1}^{K} \sum_{i=1}^{N} \|g_i^{(j)} - c_j\|^2 \tag{7}$$

where $g_i^{(j)}$ is a data point of cluster j, c_j is the cluster center, and d is an indicator of the distance of the N data points from their respective cluster centers. The number of identified clusters K is not automatically selected by the algorithm, but predefined before running it. For this reason, the clustering is performed for each parameter or combination several times for a number of clusters ($\sharp K$) varying from 2 to 4. We fixed the highest number of clusters to test at 4 because AF organization has been generally subdivided in three or four different levels by earlier accepted invasive studies [10], [11]. Conversely, 2 was considered as the smallest reasonable number of clusters, since 1 means no clustering. Then, the quality of the clustering provided by each parameter or combination is assessed through a suitable criterion, named Silhouette [25]. This is one of the most popular and widely accepted measures in the literature to assess the success of clustering process [26]. Silhouette is defined in the following manner. For each object $x \in C_i$, let $a(x)$ be the average distance of x from all other objects in cluster C_i. For every other cluster $C \neq C_i$, let $\delta(x, C)$ be the average distance of x from the objects in C. After computing $\delta(x, C)$ for all clusters $C \neq C_i$, let $b(x)$ be the smallest. The cluster for which this minimum is attained is called the neighbor of x. The number $S(x)$ is given by

$$S(x) = \frac{b(x) - a(x)}{\max(a(x), b(x))} \tag{8}$$

and provides a measure of how well object x fits into cluster C_i rather than the neighboring cluster. If $S(x)$ is close to 1, object x can be said to be well classified. If $S(x)$ is close to 0, it is unclear whether x should belong to cluster C_i or to its neighbor. A negative value suggests that x has been misclassified. The average silhouette width of a clustering ($\bar{S}$) is the arithmetic mean of the silhouette value of all objects in the dataset. A value of Silhouette $\bar{S}$ has been calculated for each parameter or combination, and for each $\sharp K$. Moreover, each $\bar{S}$ value has been calculated averaging all the 14 values of $\bar{S}$ obtained on the dataset at our disposal by a procedure reminiscent of the one-leave one-out technique [27], as follows: each $\bar{S}$ has been calculated as its average obtained leaving out one patient at a time and evaluating the clustering on the remaining 13.

Finally, the clusters associated with the parameter or combination showing the highest performance (highest $\bar{S}$) are selected for further analysis, just in terms of cluster discriminatory quality, without any kind of subjective physiological interpretation. Mean values of spatial complexity $k_{0.95}$ and temporal stationarity $\text{NMSE}_{k=3}$ are calculated for each cluster. Additionally, the level of significant difference among the obtained clusters is also evaluated for the variances of the selected parameter or combination over all the segments, further to its mean values, already exploited for the clustering. A significant result would strengthen further differences among the clusters already highlighted for their mean values. Results in terms of average complexity of the different clusters are then compared with earlier invasive studies, in order to suggest possible analogies between them and to hazard a possible physiological interpretation, suggesting they can be considered as a marker of reflection of the AF organization type on the surface ECG.

G. Statistical Analysis

Mean values of parameter $k_{0.95}$ have been calculated for each patient averaging its values over segments $s = 1, \ldots, 6$. Mean values of parameters $\text{NMSE}_{k_{0.95}}$ and $\text{NMSE}_{k=3}$ have been calculated for each patient averaging their values over segments $s = 2, \ldots, 6$. Pearson's correlation coefficient r is calculated for each relation analyzed in the study. Statistical significances have been evaluated by means of Welch's t-test.

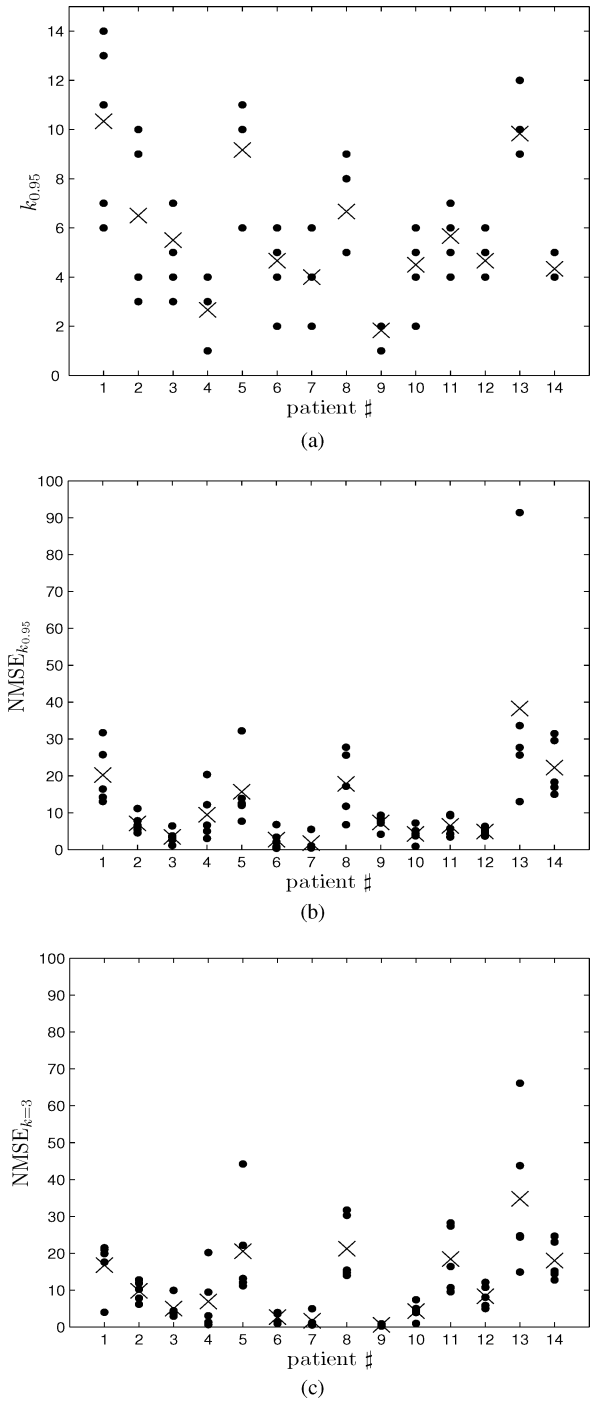

Fig. 4. Values of each parameter in segments 2–6 for each analyzed patient (•); mean values are also shown for each patient (×). (a) Values of $k_{0.95}$. (b) Values of $\mathrm{NMSE}_{k_{0.95}}$. (c) Values of $\mathrm{NMSE}_{k=3}$. Note that $k_{0.95}$ is an integer and dots can sometimes overlap.

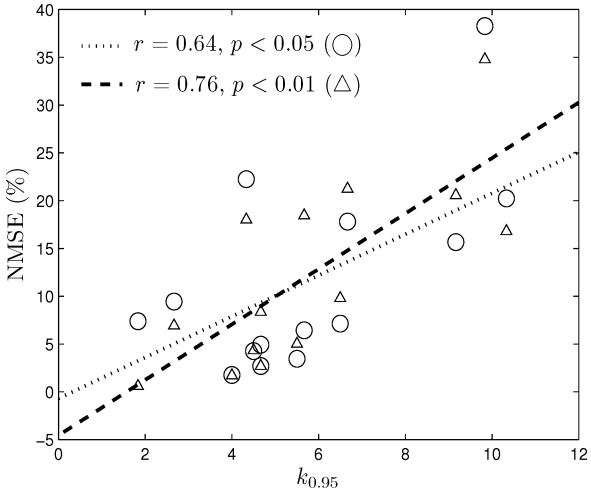

Fig. 5. Results of the spatio-temporal organization analysis $\mathrm{NMSE}_{k_{0.95}}$ versus $k_{0.95}$ (◯) and $\mathrm{NMSE}_{k=3}$ versus $k_{0.95}$ (△). Dotted line summarizes the linear regression of $\mathrm{NMSE}_{k_{0.95}}$ versus $k_{0.95}$. Dashed line summarizes the linear regression of $\mathrm{NMSE}_{k=3}$ versus $k_{0.95}$. Values of the correlation coefficients r and their significance p for each analysis are also reported.

III. Results

A. Spatio-temporal Organization of the AA During AF

Fig. 4(a)–(c) shows the values of parameters $k_{0.95}$, $\mathrm{NMSE}_{k_{0.95}}$, and $\mathrm{NMSE}_{k=3}$, respectively, in segments 2–6 for each analyzed patient (•), reporting also the mean value for each patient (×). Notice the differences in the mean values and in the variances for the different patients.

The results of the spatio-temporal organization analysis are presented in Fig. 5. Both analyses $\mathrm{NMSE}_{k_{0.95}}$ versus $k_{0.95}$ (◯) and $\mathrm{NMSE}_{k=3}$ versus $k_{0.95}$ (△) are shown, together with the values of the correlation coefficients r and significance p for each analysis. Mean values of parameters $k_{0.95}$, $\mathrm{NMSE}_{k_{0.95}}$, and $\mathrm{NMSE}_{k=3}$ have been calculated for each patient as explained in Section II-G.

Correlation coefficient $r = 0.64$ (>0.05) for the analysis $\mathrm{NMSE}_{k_{0.95}}$ versus $k_{0.95}$ (◯) underlines a positive correlation between the two parameters, which is representative of the ensemble of the data ($p < 0.05$), as reported in Fig. 5. This positive correlation points out the inverse correlation between stationarity and complexity, hypothesized in Section II-E. Selecting the $k = 3$, most significant topographies of the initial segment, as introduced in Section II-E2, the average reconstruction errors ($\mathrm{NMSE}_{k=3}$) across the remaining segments between the data in the original segments and their projections increased generally in patients presenting higher complexity ($k_{0.95} > 4$), as shown by the analysis $\mathrm{NMSE}_{k=3}$ versus $k_{0.95}$ (△). The significant increase in the correlation of the two parameters is underlined by the reciprocal increase in the correlation coefficient $r = 0.76$ ($p < 0.01$), as reported in Fig. 5. AA signal reconstruction is generally better for signals showing low complexity. No significant correlation was found between both $k_{0.95}$ and $\mathrm{NMSE}_{k=3}$, respectively, with the energy of the segments. Again, no significant correlation was found between the difference $\mathrm{NMSE}_{k_{0.95}} - \mathrm{NMSE}_{k=3}$ and $k_{0.95}$.

B. Cluster Analysis

Results of the cluster analysis as introduced in Section II-F are summarized in Table I.

The parameter showing the highest performance is $\mathrm{NMSE}_{k_{0.95}}$ (0.761) with a number of classes equals to 3.

TABLE I
CLUSTERING QUALITY ASSESSMENT THROUGH AVERAGE SILHOUETTE WIDTH OF CLUSTERINGS $\bar{S}$

Clustering parameters	$\sharp K = 2$	$\sharp K = 3$	$\sharp K = 4$
$k_{0.95}$	0.679	0.637	**0.687**
$\text{NMSE}_{k_{0.95}}$	0.677	**0.761**	0.645
$k_{0.95}$ & $\text{NMSE}_{k_{0.95}}$	0.643	0.681	0.534
$\text{NMSE}_{k=3}$	**0.700**	0.741	0.665
$k_{0.95}$ & $\text{NMSE}_{k=3}$	0.642	0.691	0.550

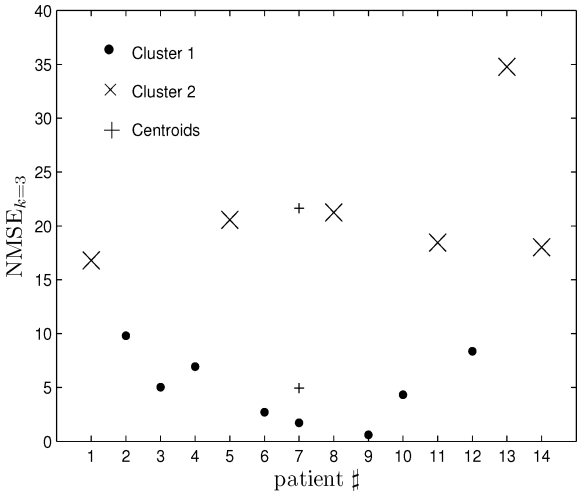

Fig. 6. Cluster analysis based on parameter $\text{NMSE}_{k=3}$ with $\sharp K = 2$. Cluster 1 (•) is characterized by low complexity and high stationarity across the BSPM recording (or low $\text{NMSE}_{k=3}$), while Cluster 2 (×) is characterized by higher complexity and lower stationarity (higher $\text{NMSE}_{k=3}$).

However, for the same number of classes, $\text{NMSE}_{k=3}$ shows a very similar value (0.741). Looking at the provided clusters, we noticed that the two clustering differed for just one object differently classified (patient ♯11), and that both were characterized by having a cluster containing only one object (the same for both, patient ♯13). Looking at Fig. 4(b) and (c), we can notice that patient ♯13 is the one showing the highest value of NMSE in both cases. Moreover, its segments are characterized by values of $\text{NMSE}_{k_{0.95}}$ and $\text{NMSE}_{k=3}$ noticeably overlapping the ones of the other patients (see Fig. 4(b) and (c), respectively; this observation is particularly evident for $\text{NMSE}_{k_{0.95}}$). Therefore, we found it reasonable to move patient ♯13 to the cluster gathering the highest values of NMSE, thus considering $\sharp K = 2$. In this scenario, it can be noticed that $\text{NMSE}_{k=3}$ is the parameter appearing as the most discriminant, since associated with the highest value of $\bar{S} = 0.700$ (first column of Table I). Hence, $\text{NMSE}_{k=3}$ is the parameter selected for further analysis. Fig. 6 shows the output of the clustering based on $\text{NMSE}_{k=3}$, with $\sharp K = 2$. As can be noticed, one cluster (•) is characterized by low complexity and high stationarity (or repetitiveness of the PCA mixing matrix) across the BSPM recording (low $\text{NMSE}_{k=3}$), while the second (×) is characterized by higher complexity and lower stationarity (higher $\text{NMSE}_{k=3}$).

Table II summarizes the statistics of parameters $k_{0.95}$ and $\text{NMSE}_{k=3}$ (mean ± SD) for each cluster obtained exploiting

TABLE II
MEAN PARAMETER VALUES FOR AA SPATIO-TEMPORAL ANALYSIS, FOR $\sharp K = 2$

Parameter	Cluster 1	Cluster 2	p-value
$k_{0.95}$	4.29±1.49	7.67±2.46	$p < 0.01$
$\text{NMSE}_{k=3}$	4.94±3.25	21.64±6.64	$p < 10^{-4}$

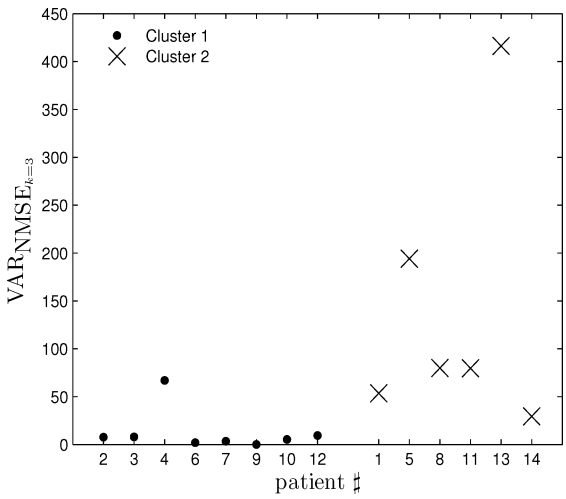

Fig. 7. Variances of parameter $\text{NMSE}_{k=3}$ over all segments in the same patient, grouped according to cluster analysis based on $\text{NMSE}_{k=3}$ in order to visually emphasize the significant difference between the two subgroups of patients.

$\text{NMSE}_{k=3}$. Rounded numbers of $k_{0.95}$ are 4 for the first cluster (range 2–7) and 8 for the second cluster (range 4–10).

A Welch's t-test was performed on the variances of parameter $\text{NMSE}_{k=3}$ over all the AA segment recordings for each patient, grouped as in the two clusters. By means of this analysis, the differences in the variances of $\text{NMSE}_{k=3}$ values, earlier observed in Fig. 4(c), were investigated. A significant difference was observed for the variances of $\text{NMSE}_{k=3}$ between the two clusters ($p < 0.05$), as portrayed in Fig. 7. This underlines the significant difference in terms of reconstruction error, and then stationarity, between AA signals characterized by different complexity, strengthening the idea that the proposed parameters may discriminate between them.

IV. DISCUSSION

The degree of organization in the AA during AF has been observed to be related to its chronification [28], [29] and thus potentially to better lead its treatment [30]. Nonetheless, a standard noninvasive procedure to assess AF organization still lacks nowadays, despite its potential relevance in clinical decision making. This study has put forward a novel automated approach to noninvasively evaluate the degree of spatio-temporal organization in the AA during AF. A quantitative assessment of AA organization was carried out by means of PCA by assessing the spatial complexity and temporal stationarity of the wavefront patterns on the surface ECG. Complexity and stationarity were investigated through parameters $k_{0.95}$ and $\text{NMSE}_{k=3}$, respectively, evaluating the structure of the mixing matrices derived

by the PCA of the different AA segments across the BSPM recording. Two are the main results of this study, and both may already support the usefulness of these parameters in clinical applications. The first finding is the significant positive correlation between parameters $k_{0.95}$ and $\text{NMSE}_{k_{0.95}}$. This result supports the hypothesis that the level of organization of the AA signal recorded on the surface of the body during AF is related both to the complexity of its recorded electrical activity and to the tendency of its potential field spatial pattern to remain unchanged over time, showing that these two features can both be noninvasively evaluated. The second finding is the ability of the proposed parameters, and of $\text{NMSE}_{k=3}$ in particular, to produce robust clusters, which are characterized by features comparable with those obtained in earlier invasive studies on AF organization classification, thus suggesting for the first finding a physiological interpretation, and the possibility to exploit these parameters in the future for noninvasive AF organization classification.

Moreover, the absence of significant correlations of both $k_{0.95}$ and $\text{NMSE}_{k=3}$, respectively, with the energy of the segments in a BSPM recording, suggests that the influence of the noise can be considered the same in any recording, and thus, the complexity reasonably supposed to be independent of it. Again, the absence of a significant correlation between the difference $\text{NMSE}_{k_{0.95}} - \text{NMSE}_{k=3}$, and $k_{0.95}$ suggests that the increase in the correlation between NMSE and $k_{0.95}$, when fixing $k = 3$, cannot be considered as an artifact of the method.

A. Comparison With Invasive Studies

The aforementioned second finding is of particular interest because the rounded values of $k_{0.95}$ calculated for both clusters are 4 for one cluster and 8 for the other. These values are similar to those obtained by Faes *et al.* [12] (4 versus 4, respectively, 8 versus 9) when analyzing the number of components needed to represent 95% of the variance in more or less organized AF in a single-lead electrogram recording. Indeed, Faes *et al.* showed that a more organized AF can be represented by a reduced number of components (4), compared to a more disorganized AF (which needs nine components). The consistency between the results provided by the two studies, made us hypothesize an analogy between them, and therefore, suggests for them a physiological interpretation. This is, a reflection of the underlying AF organization complexity seems to be present on the surface ECG. In any case, Faes *et al.* presented a local measure of the temporal organization of AF, since they analyzed single-lead electrograms. Conversely, the present study introduced noninvasive global indices of the spatio-temporal organization of the whole AA as measured on surface recordings. Finally, it is worth noticing that the two clusters obtained through $\text{NMSE}_{k=3}$ and exploited for further analysis have been selected just in terms of clustering quality, without any kind of additional (possibly subjective) physiological priors.

B. Comparison With Noninvasive Studies

The possibility of analyzing the global activity of the atria through noninvasive recordings during AF has been widely considered [31]. The noninvasive assessment of human AF organization through Holter ECG recordings was earlier described by Alcaraz *et al.*, both in the attempt to predict the spontaneous termination of paroxysmal AF [32], and to describe the paroxysmal AF time variation [33]. However, the use of a limited number of leads could prevent the exploitation of the spatial diversity of multi-lead ECGs and might not be always representative of the voltages that can be recorded from the whole body surface. In this scenario, only the temporal information over just one or few leads is exploited, and the useful spatial information given by a multi-lead system is completely disregarded. The idea in this study is to reason more at an interlead spatial information level than at an intralead temporal information level.

A comparison with the results earlier obtained by Guillem *et al.* [14] on the same dataset was carried out, even in the absence of a gold standard for both, in order to compare two different noninvasive methodologies. Guillem *et al.* [14] performed a visual classification of AF making use of a noninvasive method based on wavefront propagation mapping, according to the same criteria and terminology for classification as those of Konings *et al.* [11], although applied to surface recordings instead of electrograms. Using the method in [14], six patients were classified as AF type I (single wavefront propagating across the body surface) and eight as AF type II/III (no observable clear wavefront or multiple wavefronts that do not propagate across the body surface observed simultaneously). In the hypothesis of considering patients classified as AF type I by Guillem as comparable to those in this study belonging to the cluster showing lower complexity (Cluster 1), and patients classified as AF type II/III as comparable to those belonging to the cluster showing higher complexity (Cluster 2), 10 out of 14 patients have been labeled in the same way by both methodologies. The comparison showed interesting similarity (10 out of 14 patient equally classified), pointing out the importance of the high spatial diversity offered by BSPM recordings. Differently classified patients might be due to the different temporal resolutions employed by the two methods. Indeed, in [14], each cycle was analyzed individually (160 ms for a typical atrial dominant cycle length, but it varies for each patient), compared with 10 s employed in this study.

C. General Remarks and Limitations

Different studies based on invasive recordings have shown that the atrial electrical activity during AF presents a significant spatial inhomogeneity [5], [34], with coexistence of atrial areas characterized by different AA organization, which is more evident in patients with paroxysmal AF [6], [12]. Particularly, in patients with chronic AF, a shortening of the AA intervals and a greater prevalence of disorganized activity in all the atrial sites examined was observed. However, in patients with paroxysmal AF, a significant dispersion of refractoriness was observed [6]. Direct correlation of our observations with these findings cannot be inferred because of the lack of simultaneous invasive recordings, so that the actual mechanisms of AF in each patient are unknown. Moreover, the dataset is composed by only persistent AF recordings. Nonetheless, it might be expected that the global

perspective on the underlying AA given by surface ECG recordings mainly reflects the behavior of the atrial areas characterized by an AF type similar to the predominant one observed on the body surface.

We investigated if the temporal length of the TQ segments (and then the RR periods) influenced the stationarity and complexity of the AA signals. No significant correlation was found. Thus, the RR periods did not bias the analysis. Moreover, even if the way TQ segments have been concatenated is rough, without any kind of smoothing or interpolation, this is not a problem for PCA. Indeed, PCA concentrates on variances, and therefore, it is based on the second-order statistics of the signals under analysis at zero time lag, i.e., the coherence between consecutive samples is ignored. Therefore, PCA is not affected by the specific temporal location of each sample, or, in other words, its results are not influenced by the fact of using temporally consecutive samples. Finally, it is worthy to notice that only the AA in the TQ segments has been considered in this study. Hence, since the QRS-T complexes have been discarded, they have no influence on the final results.

The model exploited in this study for the evaluation of the temporal stationarity of the AA topographies over the experiment is similar to the one proposed by Rieta *et al.* [35], used to corroborate the hypothesis that an AF recording satisfies the independent component analysis model, in terms of stationarity of the projection coefficients. Nonetheless, as opposed to that model, mixing matrix repetitiveness is herein analyzed in terms of similarity between the original observations and the reconstructed ones.

One limitation of this study is the absence of simultaneous electrograms in order to have an objective reference for a Koning's-like classification of the patients in different AF classes. A second limitation is that the method was applied only on the TQ segments in the BSPM recording. This was done in order to avoid interferences on the estimation of the complexity due to the presence of QRS complex residues in the remainder ECG, since a QRS-T cancellation or AA extracting method able to produce a remainder ECG free from QRS residues still does not exist. Moreover, AA extracting methods containing a first estimation based on PCA were avoided, since the analysis presented here, also based on PCA, could be in some ways biased by them. Another limitation is that this study was conducted on a reduced set of patients. Nonetheless, p-value significances of the obtained results makes them promising despite the small dataset. Again, it is proper to point out that spatial complexity and temporal stationarity are, in the context arising from the definitions provided, related concepts, and thus they can be only in part viewed as different aspects of the general concept of AF organization. Even if this study has proved that high complexity generally results in low stationarity, the possibility to observe highly complex and also highly stationary patterns remains something that has to be proven. Finally, despite the undeniable usefulness of the high spatial resolution given by BSPM recordings, the possibility to employ this analysis on standard 12-leads ECGs, more frequently needed in clinical practice, needs to be assessed in future studies. Always due to the lack of simultaneous electrograms, to future study is also left the question if the proposed parameters may be used for noninvasive AF classification, and thus the confirmation of the presence of a reflection of the AF organization on the surface ECG.

V. Conclusion

Spatio-temporal organization in the AA during AF can be noninvasively and quantitatively evaluated from BSPM recordings. This can be carried out looking at the reflection on the surface ECG of the spatial complexity of the recorded electrical activity and of the temporal stationarity of its potential field spatial pattern. We observed a significant correlation, characterized by features comparable with those obtained in earlier invasive studies on AF organization classification. Hence, automated analysis of AF organization in surface recordings is indeed possible and our results strongly support the appropriateness of signal-processing approaches exploiting spatial diversity in AF analysis. Analogies with earlier invasive studies suggest the potential of noninvasive techniques for providing physiologically meaningful results.

Acknowledgment

Authors would like to thank Dr. Bollman and Dr. Husser for their help in patient recruitment.

References

[1] G. Moe, "On the multiple wavelet hypothesis of atrial fibrillation," *Arch. Int. Pharmacodyn. Ther.*, vol. 140, pp. 83–188, 1962.

[2] M. A. Allessie, W. E. J. E. P. Lammers, F. I. M. Bonke, and J. Hollen, "Experimental evaluation of Moe's multiple wavelet hypothesis of atrial fibrillation," in *Cardiac Electrophysiology and Arrhythmias*. Orlando, FL: Grune & Stratton, 1985, 265–275.

[3] E. P. Gerstenfeld, A. V. Sahakian, and S. Swiryn, "Evidence for transient linking of atrial excitation during atrial fibrillation in humans," *Circulation*, vol. 86, pp. 375–382, 1992.

[4] G. W. Botteron and J. M. Smith, "A technique for measurement of the extent of atrial activation during atrial fibrillation in the intact human heart," *IEEE Trans. Biomed. Eng.*, vol. 42, no. 6, pp. 579–586, Jun. 1995.

[5] H. Li, J. Hare, K. Mughal, D. Krum, M. Biehl, S. Deshpande, A. Dhala, Z. Blanck, J. Sra, M. Jazayeri, and M. Akhtar, "Distribution of atrial electrogram types during atrial fibrillation: Effect of rapid atrial pacing and intercaval junction ablation," *J. Amer. Coll. Cardiol.*, vol. 27, pp. 1713–1721, 1996.

[6] F. Gaita, L. Calò, R. Riccardi, L. Garberoglio, M. Scaglione, G. Licciardello, L. Coda, P. Di Donna, P. Bocchiardo, D. Caponi, L. Antolini, F. Orzan, and G. Trevi, "Different patterns of atrial activation in idiopathic atrial fibrillation: Simultaneous multisite atrial mapping in patients with paroxysmal and chronic atrial fibrillation," *J. Amer. Coll. Cardiol.*, vol. 37, pp. 534–541, 2001.

[7] A. Bollmann, "Quantification of electrical remodeling in human atrial fibrillation," *Cardiovas. Res.*, vol. 47, pp. 207–209, 2000.

[8] V. Fuster, L. E. Ryden, D. S. Cannom, H. J. Crijns, and A. B. e. a. Curtis, "ACC/AHA/ESC 2006 guidelines for the management of patients with atrial fibrillation: A report of the American College of Cardiology/American Heart Association Task Force on practice guidelines and the European Society of Cardiology Committee for practice guidelines (writing committee to revise the 2001 guidelines for the management of patients with atrial fibrillation): Developed in collaboration with the European heart rhythm association and the heart rhythm society," *Circulation*, vol. 114, pp. e257–e354, 2006.

[9] T. H. Everett, J. R. Moorman, L. C. Kok, J. G. Akar, and D. E. Haines, "Assessment of global atrial fibrillation organization to optimize timing of atrial defibrillation," *Circulation*, vol. 103, pp. 2857–2861, 2001.

[10] J. L. Wells, R. B. Karp, N. T. Kouchoukos, W. A. H. Maclean, T. N. James, and A. L. Waldo, "Characterization of atrial fibrillation in man: Studies following open-heart surgery," *PACE*, vol. 1, pp. 426–438, 1978.
[11] K. T. Konings, C. J. Kirchhof, J. R. Smeets, H. J. Wellens, O. C. Penn, and M. A. Allessie, "High-density mapping of electrically induced atrial fibrillation in humans," *Circulation*, vol. 89, pp. 1665–1680, 1994.
[12] L. Faes, G. Nollo, M. Kirchner, E. Olivetti, F. Gaita, R. Riccardi, and R. Antolini, "Principal component analysis and cluster analysis for measuring the local organisation of human atrial fibrillation," *Med. Biol. Eng. Comput.*, vol. 39, pp. 656–663, 2001.
[13] A. Bollmann, D. Husser, L. Mainardi, F. Lombardi, P. Langley, A. Murray, J. J. Rieta, J. Millet, S. Bertil Olsson, M. Stridh, and L. Sornmo, "Analysis of surface electrocardiograms in atrial fibrillation: Techniques, research, and clinical applications," Europace, vol.8, 911–926, 2006.
[14] M. S. Guillem, A. M. Climent, F. Castells, D. Husser, J. Millet, A. Arya, C. Piorkowski, and A. Bollmann, "Noninvasive mapping of human atrial fibrillation," *J. Cardiovasc. Electrophysiol.*, vol. 24, pp. 1–7, 2009.
[15] R. L. Lux, "Electrocardiographic body surface potential mapping," *Crit. Rev. Biomed. Eng.*, vol. 8, pp. 253–279, 1982.
[16] S. J. Maynard, I. B. Menown, G. Manoharan, J. Allen, A. J. McC, and A. A. Adgey, "Body surface mapping improves early diagnosis of acute myocardial infarction in patients with chest pain and left bundle branch block," *Heart*, vol. 89, pp. 998–1002, 2003.
[17] B. Khaddoumi, H. Rix, O. Meste, M. Fereniec, and R. Maniewski, "Body Surface ECG Signal Shape Dispersion," *IEEE Trans. Biomed. Eng.*, vol. 53, no. 12 pp. 2491–2500, Dec. 2006.
[18] F. Castells, P. Laguna, L. Sörnmo, A. Bollmann, and J. M. Roig, "Principal component analysis in ecg signal processing," *EURASIP J. Appl. Signal Process.*, vol. 2007, no. 1, pp. 98–98, 2007.
[19] P. Bonizzi, R. Phlypo, V. Zarzoso, O. Meste, and A. Fred, "Atrial signal extraction in atrial fibrillation ecgs exploiting spatial constraints," presented at the *EUSIPCO*, Lausanne, Switzerland, August 25–29, 2008.
[20] P. Bonizzi, R. Phlypo, V. Zarzoso, and O. Meste, "The exploitation of spatial topographies for atrial signal extraction in atrial fibrillation ECGs," in *Proc. IEEE EMBS*, 2008, vol. 30, pp. 1867–1870.
[21] L. Sörnmo and P. Laguna, *Bioelectrical Signal Processing in Cardiac and Neurological Applications*. Amsterdam, The Netherlands: Elsevier/Academic, 2005.
[22] F. Badilini, J. Fayn, P. Maison-Blanche, A. Leenhardt, M. C. Forlini, I. Denjoy, P. Coumel, and P. Rubel, "Quantitative aspects of ventricular repolarization: Relationship between three-dimensional T wave loop morphology and scalar QT dispersion," *Ann. Noninvasive Electrocardiol.*, vol. 2, pp. 146–157, 1997.
[23] S. G. Priori, D. W. Mortara, C. Napolitano, L. Diehl, V. Paganini, and F. Cantù, G. Cantù, P. J. Schwartz, "Evaluation of the spatial aspects of T-wave complexity in the long-QT syndrome," *Circulation*, vol. 96, no. 9, pp. 3006–3012, 1997.
[24] P. M. Okin, M. Malik, K. Hnatkova, E. T. Lee, J. M. Galloway, L. G. Best, B. V. Howard, and R. B. Devereux, "Repolarization abnormality for prediction of all-cause and cardiovascular mortality in American Indians: The strong heart study," *J. Cardiovasc. Electrophysiol.*, vol. 16, pp. 945–51, 2005.
[25] L. Kaufman and P. J. Rousseeuw, *Finding Groups in Data An Introduction to Cluster Analysis*. New York: Wiley Interscience, 1990.
[26] Q. H. Nguyen and V. J. Rayward-Smith, "Internal quality measures for clustering in metric spaces," *Int. J. Bus. Intell. Data Min.*, vol. 3, no. 1, pp. 4–29, 2008.
[27] K. Fukunaga and D. M. Hummels, "Bayes error estimation using parzen and k-nn procedures," *IEEE Trans. Pattern Anal. Mach. Intell.*, vol. PAMI-9, no. 5, 634–643, Sep. 1987.
[28] G. W. Botteron and J. M. Smith, "Quantitative assessment of the spatial organization of atrial fibrillation in the intact human heart," *Circulation*, vol. 93, pp. 513–518, 1996.
[29] S. M. Al-Khatib, W. E. Wilkinson, L. L. Sanders, E. A. McCarthy, and E. L. Pritchett, "Observations on the transition from intermittent to permanent atrial fibrillation," *Amer. Heart J.*, vol. 140, pp. 142–145, 2000.
[30] T. H. Everett, L. C. Kok, R. H. Vaughn, J. R. Moorman, and D. E. Haines, "Frequency domain algorithm for quantifying atrial fibrillation organization to increase defibrillation efficacy," *IEEE Trans. Biomed. Eng.*, vol. 48 no. 9, pp. 969–978, Sep. 2001.
[31] S. Petrutiu, J. Ng, G. M. Nijm, H. Al-Angari, S. Swiryn, and A. V. Sahakian, "Atrial Fibrillation and Waveform Characterization. A Time Domain Perspective in the Surface ECG," *IEEE Eng. Med. Biol. Mag.*, vol. 25, no. 6, pp. 24–30, Nov./Dec. 2006.
[32] R. Alcaraz and J. J. Rieta, "Wavelet bidomain sample entropy analysis to predict spontaneous termination of atrial fibrillation," *Physiol. Meas.*, vol. 29, pp. 65–80, 2008.
[33] R. Alcaraz and J. J. Rieta, "Non-invasive organization variation assessment in the onset and termination of paroxysmal atrial fibrillation," *Comput. Methods Programs Biomed.*, vol. 93, pp. 148–154, 2009.
[34] F. Censi, V. Barbaro, P. Bartolini, G. Calcagnini, A. Michelucci, G. F. Gensini, and S. Cerutti, "Recurrent patterns of atrial depolarization during atrial fibrillation assessed by recurrence plot quantification," *Ann. Biomed. Eng.*, vol. 28, pp. 61–70, 2000.
[35] J. J. Rieta, C. Sánchez, J. M. Sanchis, F. Castells, and J. Millet, "Mixing matrix pseudostationarity and ECG preprocessing impact on ICA-based atrial fibrillation analysis," in *Lecture Notes in Computer Science*, vol. 3195, pp. 1079–1086, 2004.

Pietro Bonizzi was born in Milano, Italy. He received the M.Sc. in biomedical engineering from Politecnico di Milano, Milan, in 2006. He is currently working toward the Ph.D. degree at the Laboratoire d'Informatique, Signaux et Systèmes de Sophia Antipolis (I3S), France.

His research interests include biomedical signal processing, with emphasis on cardiac signals and the characterization of atrial fibrillation using blind statistical signal-processing techniques.

María de la Salud Guillem was born in Valencia, Spain. She received the M.S. degree in telecommunications engineering from Universidad Politécnica de Valencia (UPV), Valencia, in 2003, the M.S. degree in biomedical engineering and the Ph.D. degree in electronics engineering from Northwestern University, Evanston, IL, in 2006 and 2008, respectively.

She was a Fullbright Fellow at Northwestern University. She is currently an Assistant Professor in the Electronics Engineering Department, UPV, where she is also a Researcher at the Institute for Applications of Advanced Information and Communication Technologies. Her research interests include biomedical signal processing with main interest in cardiac signals.

Andreu M. Climent was born in Gandia, Spain. He received the M.S. degree in telecommunications engineering from Universidad Politécnica de Valencia (UPV), Valencia, Spain, in 2006. He is currently working toward the Ph.D. degree at the Electronics Engineering Department, UPV.

He was a Research Fellow at Magdeburg, Milan, Lund, Leipzig, and Cleveland during 2005 through 2008. He is also a Fellow Researcher at the Institute for Applications of Advanced Information and Communication Technologies, UPV. His research interests include atrioventricular conduction during supraventricular arrhythmias and biomedical signal processing.

Jose Millet was born in Valencia, Spain. He received the M.S. degree in physics from the University of Valencia, Valencia, Spain, in 1991, and the Ph.D. degree in electrical and electronic engineering from the Universidad Politécnica de Valencia (UPV), Valencia, in 1997.

He is currently a Full Professor in the Department of Electronics Engineering, UPV, where he has also been the Coordinator of the Biomedical Engineering branch, Institute for Applications of Advanced Information and Communication Technologies. His research interests include biomedical signal processing, biomedical signal acquisition and instrumentation, implantable devices for treatment of cardiac arrhythmias, and Cardiac MRI.

Vicente Zarzoso (S'94–M'03) graduated with highest distinction in telecommunications engineering from the Polytechnic University of Valencia, Valencia, Spain, in 1996. He received the Ph.D. degree from the University of Liverpool, Liverpool, U.K., in 1999, and the Habilitation to Lead Researches degree from the University of Nice-Sophia Antipolis, France, in 2009.

From 2000 to 2005, he was a Research Fellow at the Royal Academy of Engineering, U.K. Since 2005, he has been at the Computer Science, Signals and Systems Laboratory of Sophia Antipolis (I3S), France. His research interests include statistical signal and array processing and its application to biomedical problems and communications.

Francisco Castells was born in Valencia, Spain, in 1976. He received the M.Eng. degree in telecommunications engineering from Universidad Politécnica de Valencia (UPV), Valencia, in 2000, and the Ph.D. degree in electronics engineering from UPV, in 2006.

He was at Alcatel SEL AG, Germany during 2000 and 2001. He is currently a Permanent Lecturer at the Electronics Engineering Department, UPV, where he is also a Member of the institute for applications of advanced information and communication technologies. His research interests include statistical signal processing of biomedical signals, with special emphasis on the characterization and analysis of atrial fibrillation.

Olivier Meste received the M.Sc. degree in automatic and signal processing, and the Ph.D. degree in scientific engineering from the University of Nice-Sophia Antipolis, France, in 1989 and 1992, respectively.

He is currently a Full Professor at the University of Nice-Sophia Antipolis and a Researcher at the Signals and Systems Laboratory of Sophia Antipolis (I3S). His research interests include digital processing, time-frequency representations and modeling of biological signals and systems, including ECG, electromyography, and EEG.

Dr. Meste is a member of the Bio Imaging and Signal Processing Technical Committee, IEEE Signal Processing Society.